HHS Public Access

Author manuscript

Bone. Author manuscript; available in PMC 2019 August 01.

Published in final edited form as:

Bone. 2018 August ; 113: 49–56. doi:10.1016/j.bone.2018.05.005.

Association of High-resolution Peripheral Quantitative Computed Tomography (HR-pQCT) Bone Microarchitectural Parameters with Previous Clinical Fracture in Older Men: the Osteoporotic Fractures in Men (MrOS) Study

Howard A. Fink, MD, MPH[a,b,c,d], **Lisa Langsetmo, PhD**[d], **Tien N. Vo, MS**[d], **Eric S. Orwoll, MD**[e], **John T. Schousboe, MD, PhD**[f,g], and **Kristine E. Ensrud, MD, MPH**[b,c,d] **for the Osteoporotic Fractures in Men (MrOS) Study Group**

[a]Geriatric Research Education & Clinical Center, Veterans Affairs Health Care System, Minneapolis, MN, USA

[b]Center for Chronic Disease Outcomes Research, Veterans Affairs Health Care System, Minneapolis, MN, USA

[c]Department of Medicine, University of Minnesota, Minneapolis, MN, USA

[d]Division of Epidemiology and Community Health, School of Public Health, University of Minnesota, Minneapolis, MN, USA

[e]Bone and Mineral Unit, Oregon Health & Science University, Portland, OR, USA

[f]Park Nicollet Institute, Minneapolis, MN, USA

[g]Division of Health Policy and Management, University of Minnesota, Minneapolis, MN, USA

Abstract

High-resolution peripheral quantitative computed tomography (HR-pQCT) assesses both volumetric bone mineral density (vBMD) and trabecular and cortical microarchitecture. However, studies of the association of HR-pQCT parameters with fracture history have been small, predominantly limited to postmenopausal women, often performed limited adjustment for potential confounders including for BMD, and infrequently assessed strength or failure measures. We used data from the Osteoporotic Fractures in Men (MrOS) study, a prospective cohort study of

Corresponding author: Dr. Howard A. Fink, Veterans Affairs Health Center (11-G), One Veterans Drive, Minneapolis, MN 55417, USA. Phone: (612) 467-3304. Fax (612) 725-2084., howard.fink@va.gov.

Declarations of Interest: Dr. Orwoll reports grants from Merck & Company and Eli Lilly & Company unrelated to but during the conduct of this study, and consulting fees from Merck & Company unrelated to but during the conduct of this study. All other authors declare they have no conflict of interest to disclose.

Authors' Roles:
Study concept and design: HAF, ESO, KEE
Data collection: ESO, KEE
Data analysis and interpretation: TNV, LL, HAF
Drafting manuscript: HAF
Critical review and final approval of manuscript content: HAF, LL, TNV, KEE, JTS, ESO

Statistical Analysis: Mr. Tien Vo performed the statistical analyses and is independent of any commercial funder. He had full access to all the data in the study and takes responsibility for the integrity of the data and the accuracy of the data analyses.

community-dwelling men aged ≥65 years, to evaluate the association of distal radius, proximal (diaphyseal) tibia and distal tibia HR-pQCT parameters measured at the Year 14 (Y14) study visit with prior clinical fracture. The primary HR-pQCT exposure variables were finite element analysis estimated failure loads (EFL) for each skeletal site; secondary exposure variables were total vBMD, total bone area, trabecular vBMD, trabecular bone area, trabecular thickness, trabecular number, cortical vBMD, cortical bone area, cortical thickness, and cortical porosity. Clinical fractures were ascertained from questionnaires administered every 4 months between MrOS study baseline and the Y14 visit and centrally adjudicated by blinded review of radiographic reports. We used multivariate-adjusted logistic regression to estimate the odds of prior clinical fracture per 1 SD decrement for each Y14 HR-pQCT parameter. Three hundred forty-four (19.2%) of the 1794 men with available HR-pQCT measures had a confirmed clinical fracture between baseline and Y14. After multivariable adjustment, including for total hip areal BMD, decreased HR-pQCT finite element analysis EFL for each site was associated with significantly greater odds of prior confirmed clinical fracture and major osteoporotic fracture. Among HR-pQCT parameters, decreased cortical area appeared to have the strongest independent association with prior clinical fracture. Future studies should explore associations of HR-pQCT parameters with specific fracture types and risk of incident fractures and the impact of age and sex on these relationships.

Keywords

fracture; male; aged; radiology; bone microarchitecture

1. Introduction

Although dual-energy X-ray absorptiometry (DXA) areal bone mineral density (aBMD) is a strong predictor of future fractures, most older adults who experience fractures do not have osteoporotic aBMD. It has been postulated that this insensitivity of DXA aBMD for individual fracture prediction could be at least in part attributable to its limited ability to capture important properties of bone that confer susceptibility to fracture. High resolution peripheral quantitative computed tomography (HR-pQCT) can noninvasively assess volumetric BMD (vBMD) and microarchitectural properties of specific skeletal compartments (i.e. cortical and trabecular), and can be used to estimate bone strength.

Many cross-sectional and retrospective studies have evaluated the association of HR-pQCT parameters with odds of prior fracture in adults.[1–17] A common limitation of these studies has been their small numbers of fractures (i.e., <100),[1–4, 6, 8, 10–12] including in all but one of the studies that include men.[2, 6–8, 11] Many prior studies evaluated HR-pQCT measures at only one skeletal site[2, 6, 9, 11, 12] and didn't evaluate any HR-pQCT derived strength or failure measures.[2–6, 8, 10, 11, 13, 15, 17] Another common limitation was use of unadjudicated self-reported fractures.[1, 4, 5, 10, 14] In addition, many studies performed only limited adjustment for potentially confounding variables including none for BMD.[1, 2, 4, 6–12, 14, 16]

The present study utilizes data from the multi-site Osteoporotic Fractures in Men (MrOS) study. Its aim is to examine, in a large cohort of older men, the association of HR-pQCT

microarchitectural parameters and derived strength estimates from three skeletal sites on prospectively identified and adjudicated, but previously occurring clinical fractures. Further, analyses seek to evaluate whether observed associations are independent of potentially confounding variables including aBMD.

2. Materials and Methods

2.1. Participants

5,994 community-dwelling men aged ≥65 years were recruited from population-based listings to participate in the MrOS prospective cohort study between March 2000 and April 2002 at six U.S. sites: Birmingham, AL; Minneapolis, MN; Palo Alto, CA; Monongahela Valley near Pittsburgh, PA; Portland, OR; and San Diego, CA. MrOS exclusion criteria included inability to walk without assistance from another person, a history of bilateral hip replacement, inability to consent, or expected survival of less than six months. Institutional review boards at all participating centers approved the study protocol and written informed consent was obtained from all participants. The MrOS study design and recruitment have been described in detail elsewhere.[18, 19]

Among all MrOS enrollees, 2,424 attended the Year 14 study visit (May 2014 to May 2016) (mean of 14.2 ± 0.6 SD years after baseline), of whom 1,794 completed HR-pQCT measurements at either distal radius or at proximal (diaphyseal) or distal tibia. 1,702 men had evaluable measures at the distal radius, 1,499 had evaluable measures at the diaphyseal tibia, and 1,717 had evaluable measures at the distal tibia (Figure).

2.2. HR-pQCT Measurement

Centrally trained operators used XtremeCT II scanners to obtain 1 cm cross-sectional HR-pQCT images (nominal voxel size 61μm) of the distal radius (9 mm proximal to distal articular surface), diaphyseal tibia (30% offset) and distal tibia (22 mm proximal to the distal articular surface) (Scanco Medical AG, Brüttisellen, Switzerland).[20, 21] The non-dominant radius and ipsilateral tibia were scanned unless the participant reported a history of fracture in those locations, metal implant or shrapnel near those locations, or recent full unloading of that tibia for >6 weeks, in which case the dominant sides were scanned. Centralized quality assurance and standard analysis of all image data was performed. A central observer read all images for motion artifacts and used an established semi-quantitative 5-point grading system (1=superior, 5=poor) to score image quality; images that were graded 4 or 5 (3% of total) were judged of insufficient quality and were excluded from the analytic data set.[22] All participants with outliers (difference from cohort mean for any measure of greater than 3 standard deviations) were reviewed and those with abnormal anatomic findings at a given skeletal site (unreported fracture, metal implants or shrapnel, large osteolytic lesions, severe inflammatory arthritis with degenerative changes, or large intra-osseal injuries with ossification) were excluded from the analysis at that skeletal site. A single density cross-calibration phantom was circulated between all study sites;[23] because inter-scanner variability was <0.6%, data from the different study sites was pooled without transformations. Each clinic scanned a copy of this same phantom daily to monitor for bone density deviations exceeding 8 mg HA/cm^3 and correction factors for longitudinal changes

were applied to participant data as appropriate. Automated processes were developed to segment the radius and tibia into cortical and trabecular components. Segmentation failures were detected automatically by measuring slice-wise variation in total cross-sectional area; cases with an absolute slice-wise difference of 4mm^2 (<6% of cases) were visually reviewed and manually corrected. Linear elastic micro-finite element analysis (μFEA) then was performed, in which images were converted to a mesh of isotropic hexahedral elements using a voxel conversion technique[24] and each element was assigned an elastic modulus of 10 GPa and a Poisson's ratio of 0.3.[25] Cortical and trabecular bone were labeled as different materials, with identical material properties to facilitate calculation of compartmental load distribution. An iterative solver (Scanco FE Software v1.12, Scanco Medical) was used to compute reaction forces at the superior and inferior ends of the sections for a prescribed uniaxial 1% compressive strain. Finally, the failure load was estimated (EFL) by calculation of the reaction force at which 7.5% of the elements exceed a local effective strain of 0.7%.[25] The model computations were performed at the UCSF/QB3 Shared Computing Facility.

2.3. Ascertainment of Clinical Fractures

Beginning at MrOS baseline, incident clinical vertebral and non-vertebral fractures were identified from participant (or, if deceased, participant's contacts) responses to every four-month mail or phone queries about new fractures. More than 99% of these attempted contacts were completed among active surviving participants through a mean of 14.2 ± 0.6 SD years of follow-up. Incident non-vertebral fractures were centrally confirmed by study physician review of community radiographic reports. Incident clinical vertebral fractures were defined by both 1) presence of symptoms suggestive of vertebral fracture (e.g., back pain) that prompted the participant to seek medical attention in the community and 2) a community imaging study (e.g., radiograph, computed tomography) centrally reviewed by a masked study physician that showed a ≥1 increase in semiquantitative (SQ) grade compared to the same thoracic or lumbar vertebrae on the baseline study radiograph.[26] Incident major osteoporotic fractures were defined as any incident hip, wrist, humerus or clinical vertebral fracture.

2.4. Other Measurements

Date of birth, race (white vs. nonwhite), smoking status (ever vs. never) and self-reported fractures since age 50 were reported at MrOS baseline. Other variables were assessed at the Year 14 study visit. These included self-reported falls in the past year (any vs. none), and current alcohol use (none, 1–13, or ≥14 drinks per week). Physical activity was measured using the Physical Activity Scale for the Elderly (PASE) score.[27] Study staff measured each participant's height (stadiometer) and weight in light clothing (balance beam or digital scale). aBMD (g/cm^2) was measured at the right hip using dual x-ray absorptiometry (DXA) (QDR4500W, Hologic, Inc., Waltham, MA), unless the participant reported a right hip replacement or metal objects in the right leg, in which case the left hip was measured. MrOS DXA quality assurance measures have been detailed previously.[19] Common phantoms were used to estimate between-clinic variability in DXA measures; because variability across clinics was limited (<0.6%), cross-calibration correction factors were not required.

2.5. Statistical Analyses

Differences in baseline characteristics between men who were and were not included in the Year 14 study visit HR-pQCT analysis cohort, and differences in Year 14 characteristics between men who had and did not have a confirmed clinical fracture between MrOS baseline and the Year 14 study visit were assessed using chi-square tests or Fisher's exact test for categorical data and t-tests or ANOVA for continuous data.

A priori, we selected the finite element analysis (FEA) estimated failure loads for distal radius, diaphyseal tibia and distal tibia as our primary HR-pQCT exposure variables. Our secondary exposure variables for each of these skeletal sites were total vBMD, total bone area, trabecular vBMD, trabecular bone area, trabecular thickness, trabecular number, cortical vBMD, cortical bone area, cortical thickness, and cortical porosity. We performed logistic regression analyses to estimate the odds of confirmed clinical fracture since MrOS baseline per 1 SD decrement for each Year 14 study visit HR-pQCT parameter, calculating odds ratios (OR) and 95% confidence intervals (CI). All models first were adjusted for Year 14 age, race, clinic site, and limb length (Model 1), and then additionally were adjusted for Year 14 total hip aBMD (Model 2), and for height, weight, physical activity, smoking history, alcohol consumption, past falls, and self-reported history of fractures between age 50 and MrOS baseline (Model 3). These analyses were repeated for the outcome of confirmed major osteoporotic fracture since MrOS baseline.

In a series of sensitivity analyses, we examined: (1) fracture site-specific associations (age-adjusted associations of the microarchitectural parameters with the separate outcomes of confirmed hip, clinical vertebral, and nonhip nonvertebral fractures since MrOS baseline); (2) more recent fractures (fully adjusted analyses limited to prior clinical fractures between the Year 7 and Year 14 study visits [mean interval 7.4 ± 0.3 SD years]), (3) nontraumatic fractures (fully adjusted analyses limited to prior clinical fractures that occurred after a fall from standing height or less or otherwise were classified as minimally traumatic), and (4) "dose-related" associations (results in men with at least two prior clinical fractures and men with only one prior clinical fractures were separately compared to those in men with no fracture).

All significance levels reported were two-sided and analyses were conducted using SAS version 9.4 (SAS Institute Inc, Cary, NC).

3. Results

Compared to men not included in the Year 14 HR-pQCT analysis cohort, the 1794 men in the analysis cohort were younger, taller, heavier, more physically active, were less likely to have fallen in the past year or to have had a fracture since age 50, had higher total hip aBMD, and less frequently had a clinical fracture between baseline and the Year 14 study visit (Supplementary Table 1).

Within the HR-pQCT analysis cohort, 344 (19.2%) men had at least one confirmed clinical fracture between baseline and the Year 14 study visit, including 30 (1.7%) whose first confirmed clinical fracture was a hip fracture, 39 (2.2%) with a first clinical vertebral

fracture, and 275 (15.3%) with a first non-hip, non-vertebral fracture. Among the men with a nonhip nonvertebral fracture, the most common were ribs (n=60), ankle (n=41), foot/metatarsal (n=19), distal radius (n=18), fingers (n=18), clavicle (n=14), pelvis (n=13), face (n=13), humerus (n=11), toes (n=11), and hand (n=11). Unadjusted microarchitectural parameters are compared between men with and without a history of confirmed clinical fracture between MrOS baseline and the Year 14 study visit in Supplementary Table 2. Compared to men without fractures, those with at least one confirmed fracture were older, less physically active, were more likely to have fallen in the past year, had lower total hip aBMD, and were more likely to have reported a fracture between age 50 and MrOS baseline (Table 1).

In models adjusted for age, race, clinic site, and same bone limb length, each SD decrement in Year 14 study visit μFEA EFL was associated with an approximately 60% higher likelihood of any confirmed clinical fracture since MrOS baseline (distal radius EFL: OR, 1.62 [95% CI, 1.41–1.86]; diaphyseal tibia EFL: OR, 1.61 [1.38–1.87]; distal tibia EFL: OR, 1.61 [1.40–1.84]) (Table 2). By comparison, the association of each SD decrement in μFEA EFL with confirmed major osteoporotic fracture since MrOS baseline appeared somewhat stronger (distal radius EFL: OR, 1.74 [95% CI, 1.38–2.20]; diaphyseal tibia EFL: OR, 1.60 [1.27–2.00]; distal tibia EFL: OR, 1.94 [1.55–2.42]) (Table 3). Results for all these outcomes were somewhat attenuated after further adjustment for total hip aBMD, but persisted.

In fully adjusted models, results remained statistically significant for any confirmed clinical fracture at all sites, with an approximately 30% higher likelihood of fracture since MrOS baseline for each 1 SD decrement in EFL (distal radius EFL: OR, 1.35 [1.14–1.60]; diaphyseal tibia EFL: OR, 1.35 [1.12–1.62]; distal tibia EFL: OR, 1.26 [1.05–1.51]) (Table 2). For confirmed major osteoporotic fracture, fully adjusted results remained statistically significant at both distal sites (distal radius EFL: OR, 1.44 [1.09–1.90]; distal tibia EFL: OR, 1.51 [1.13–2.02]), but were no longer significant for diaphyseal tibia EFL (OR, 1.23 [0.94–1.62]) (Table 3).

In multivariable-adjusted analyses evaluating the association of other microarchitectural parameters, including adjustment for total hip aBMD, odds of any confirmed clinical fracture since MrOS baseline were most consistently increased per 1 SD decrement of cortical area and cortical thickness (Table 2). Decrements in total vBMD and cortical vBMD at the distal radius and distal tibia sites, but not at the diaphyseal tibia, were associated with an increased odds of prior clinical fracture. Decrements in trabecular vBMD and trabecular number at the distal radius but not at the distal tibia were associated with an increased odds of prior fracture. Cortical porosity, trabecular area and trabecular thickness were not associated with history of prior clinical fracture. Patterns of association of these microarchitectural parameters with the outcome of major osteoporotic fracture (Table 3) appeared similar to their associations with any prior clinical fracture.

In sensitivity analyses adjusted only for age due to the small number of events, the strength of association of microarchitectural parameters with past hip and clinical vertebral fractures appeared stronger than those with nonhip nonvertebral fracture (Supplementary Table 3). Fully adjusted results for confirmed clinical fractures in the most recent seven years were

similar to overall results. This was the case both for the more recent clinical fractures from any site (distal radius EFL: OR, 1.37 [1.09–1.74]; diaphyseal tibia EFL: OR, 1.22 [0.96–1.56]; distal tibia EFL: OR, 1.45 [1.12–1.87]) and for the more recent major osteoporotic fractures (distal radius EFL: OR, 1.43 [1.08–1.90]; diaphyseal tibia EFL: OR, 1.25 [0.94–1.65]; distal tibia EFL: OR, 1.50 [1.11–2.01]). In analyses excluding the 158 men with traumatic clinical fractures, findings were similar to overall results, though odds ratios appeared slightly larger and confidence intervals were wider (Supplementary Table 4). Last, when compared to men who had no confirmed clinical fracture since MrOS baseline, the fully-adjusted associations of the microarchitectural parameters with at least two confirmed past clinical fractures appeared similar to those in men with a single confirmed past clinical fracture (Supplementary Table 5).

4. Discussion

In this cohort of community-dwelling older men, lower HR-pQCT FEA estimated failure loads for distal radius, diaphyseal tibia and distal tibia were associated with significantly greater odds of prior confirmed clinical fracture and confirmed major osteoporotic fracture. These associations were independent of aBMD and multiple potentially confounding variables. Next to estimated failure load, decreased cortical area was the HR-pQCT parameter that appeared to have the strongest association with history of prior clinical fracture. In contrast, cortical porosity, trabecular area, and trabecular thickness most consistently had no association with previous clinical fracture and results for other HR-pQCT parameters were mixed. Associations with hip and clinical vertebral fractures appeared stronger than those with nonhip nonvertebral fractures. However, results appeared similar to overall when considering only prior fractures within the past seven years, when excluding traumatic fractures, and when considering associations between single or multiple fractures.

Total hip aBMD was the variable that most attenuated the associations of HR-pQCT microarchitectural parameters and FEA estimated failure load with odds of prior clinical fracture. Therefore, it is unknown whether the associations between HR-pQCT parameters and prior fracture observed in earlier studies that either did not account for BMD at all[1, 2, 4, 6–12, 14] or only did so selectively[16] are independent of the known association of BMD with fracture. In five studies that accounted for BMD, none estimated strength or failure load;[3, 5, 13, 15, 17] otherwise, our results for associations with HR-pQCT parameters were partially consistent with the BMD-adjusted results from these studies. Whereas we found that decreased cortical area at all three measured bone sites was associated with a significant aBMD-adjusted increased odds of prior clinical fracture, just one of three earlier studies that reported this measure found that a decrease was associated with an increased odds of prior fracture.[3, 5, 15] Whereas we found an increased BMD-adjusted odds of prior clinical fractures associated with decreased total bone area, total vBMD, cortical vBMD and cortical thickness at one or two of the three measured bone sites, prior studies also reported mixed results for associations between these HR-pQCT parameters and odds of past fracture.[3, 5, 13, 15, 17] Whereas we found an association of trabecular vBMD and trabecular thickness with odds of past fracture only at the distal radius and found no association between cortical porosity at any bone site and odds of past fracture, earlier

BMD-adjusted studies reported mixed results with these measures.[3, 5, 13, 15, 17] The reasons for these heterogeneous results are uncertain, but they may be attributable at least in part to between-study differences in sex, age, and the types of fractures examined. Four of these BMD-adjusted studies were in older women (range of mean ages 66 to 78 years)[3, 5, 13, 15] and one was in younger men than those in our study (mean age 70 vs. 84 years).[17] Types of prevalent fracture reported included confirmed hip fracture,[3] confirmed[13] and unconfirmed[5, 17] clinical fracture, and radiographic vertebral fracture.[15, 17]

Our findings were consistent with those from four prospective studies that all reported that FEA estimated failure load was associated with a BMD-adjusted increased risk of incident clinical fracture.[28–31] While our study found that lower cortical area at each of three skeletal sites was associated with an increased BMD-adjusted odds of prior clinical fracture, three of four prospective studies reported a BMD-adjusted association of lower cortical area at the only measured site or at both distal sites with increased risk of incident clinical fractures. Both our study and prior prospective studies showed mixed results suggesting that lower total and trabecular vBMD each are positively associated with fracture after adjustment for aBMD. Though the directions of these associations appear generally similar, the magnitudes of BMD-adjusted HR-pQCT associations with incident fracture appear larger than the associations we found in our study with the outcome of prior fracture. This might be explained by selective loss to follow-up of participants with prior clinical fractures – men who did not complete HR-pQCT measurements and therefore were not included in our analysis cohort were more likely to have had a clinical fracture between MrOS baseline and the Year 14 visit than those who completed HR-pQCT measurements. This could have biased results toward the null, underestimating the true magnitude of the association between HR-pQCT measures and odds of fracture.

The current study has several important strengths, including its enrollment of a large cohort of community-dwelling older men. An additional strength is the complete follow-up for clinical fractures between MrOS baseline and the Year 14 study visit, and central adjudication of incident fracture reports. Further, analyses were adjusted for multiple potential confounders and for areal total hip BMD.

These analyses also have several limitations. First, although fractures were prospectively identified and adjudicated, they occurred before the HR-pQCT measurements, making it impossible to determine the direction of any potential causal association. Second, as noted above, exclusion from analyses of men without HR-pQCT measurements, who were more likely to be less healthy, could have biased results toward the null. Third, there were only a small number of men with individual fracture types, so, for example, we had limited ability to evaluate the independence of associations between HR-pQCT parameters and odds of past hip and clinical vertebral fractures. Fourth, because we examined a large number of associations, particularly for secondary predictors, this increased the likelihood that statistically significant findings could have been attributable to type I error. Finally, because MrOS participants are community-dwelling, largely healthy older men, our findings may have limited applicability to other populations.

In conclusion, HR-pQCT derived estimated failure load and select other HR-pQCT parameters at multiple skeletal sites identified older men at high odds for past clinical fracture independent of both areal BMD and numerous other potentially explanatory factors. These results suggest the potential of noninvasive bone microarchitectural measures to enhance fracture prediction in this population beyond that from DXA and other clinical measures. However, these results are retrospective and need to be confirmed in prospective studies.

Supplementary Material

Refer to Web version on PubMed Central for supplementary material.

Acknowledgments

Source of Funding:

The Osteoporotic Fractures in Men (MrOS) Study is supported by National Institutes of Health funding. The following institutes provide support: the National Institute on Aging (NIA), the National Institute of Arthritis and Musculoskeletal and Skin Diseases (NIAMS), the National Center for Advancing Translational Sciences (NCATS), and NIH Roadmap for Medical Research under the following grant numbers: U01 AG027810, U01 AG042124, U01 AG042139, U01 AG042140, U01 AG042143, U01 AG042145, U01 AG042168, U01 AR066160, and UL1 TR000128.

This manuscript also is the result of work supported with resources and use of facilities of the Minneapolis VA Health Care System. The contents herein do not represent the views of the U.S. Department of Veterans Affairs or the United States Government.

Sponsor's Role: The funding agencies had no direct role in the conduct of the study; the collection, management, analyses and interpretation of the data; or preparation or approval of the manuscript.

References

1. Ackerman KE, Cano Sokoloff N, DENMG, Clarke HM, Lee H, Misra M. Fractures in Relation to Menstrual Status and Bone Parameters in Young Athletes. Med Sci Sports Exerc. 2015; 47(8):1577–86. [PubMed: 25397605]
2. Sundh D, Mellstrom D, Nilsson M, Karlsson M, Ohlsson C, Lorentzon M. Increased Cortical Porosity in Older Men With Fracture. J Bone Miner Res. 2015; 30(9):1692–700. [PubMed: 25777580]
3. Sundh D, Nilsson AG, Nilsson M, Johansson L, Mellstrom D, Lorentzon M. Increased cortical porosity in women with hip fracture. Journal of internal medicine. 2017; 281(5):496–506. [PubMed: 28097725]
4. Boutroy S, Bouxsein ML, Munoz F, Delmas PD. In vivo assessment of trabecular bone microarchitecture by high-resolution peripheral quantitative computed tomography. J Clin Endocrinol Metab. 2005; 90(12):6508–15. [PubMed: 16189253]
5. Boutroy S, Khosla S, Sornay-Rendu E, Zanchetta MB, McMahon DJ, Zhang CA, Chapurlat RD, Zanchetta J, Stein EM, Bogado C, Majumdar S, Burghardt AJ, Shane E. Microarchitecture and Peripheral BMD are Impaired in Postmenopausal White Women With Fracture Independently of Total Hip T-Score: An International Multicenter Study. J Bone Miner Res. 2016; 31(6):1158–66. [PubMed: 26818785]
6. Edwards MH, Robinson DE, Ward KA, Javaid MK, Walker-Bone K, Cooper C, Dennison EM. Cluster analysis of bone microarchitecture from high resolution peripheral quantitative computed tomography demonstrates two separate phenotypes associated with high fracture risk in men and women. Bone. 2016; 88:131–7. [PubMed: 27130873]
7. Farr JN, Khosla S, Achenbach SJ, Atkinson EJ, Kirmani S, McCready LK, Melton LJ 3rd, Amin S. Diminished bone strength is observed in adult women and men who sustained a mild trauma distal

forearm fracture during childhood. J Bone Miner Res. 2014; 29(10):2193–202. [PubMed: 24753047]

8. Klingberg E, Lorentzon M, Gothlin J, Mellstrom D, Geijer M, Ohlsson C, Atkinson EJ, Khosla S, Carlsten H, Forsblad-d'Elia H. Bone microarchitecture in ankylosing spondylitis and the association with bone mineral density, fractures, and syndesmophytes. Arthritis Res Ther. 2013; 15(6):R179. [PubMed: 24517240]
9. Christen D, Melton LJ 3rd, Zwahlen A, Amin S, Khosla S, Muller R. Improved fracture risk assessment based on nonlinear micro-finite element simulations from HRpQCT images at the distal radius. J Bone Miner Res. 2013; 28(12):2601–8. [PubMed: 23703921]
10. Bjornerem A, Bui QM, Ghasem-Zadeh A, Hopper JL, Zebaze R, Seeman E. Fracture risk and height: an association partly accounted for by cortical porosity of relatively thinner cortices. J Bone Miner Res. 2013; 28(9):2017–26. [PubMed: 23520013]
11. Jamal S, Cheung AM, West S, Lok C. Bone mineral density by DXA and HR pQCT can discriminate fracture status in men and women with stages 3 to 5 chronic kidney disease. Osteoporos Int. 2012; 23(12):2805–13. [PubMed: 22297732]
12. Melton LJ 3rd, Riggs BL, Keaveny TM, Achenbach SJ, Hoffmann PF, Camp JJ, Rouleau PA, Bouxsein ML, Amin S, Atkinson EJ, Robb RA, Khosla S. Structural determinants of vertebral fracture risk. J Bone Miner Res. 2007; 22(12):1885–92. [PubMed: 17680721]
13. Sornay-Rendu E, Boutroy S, Munoz F, Delmas PD. Alterations of cortical and trabecular architecture are associated with fractures in postmenopausal women, partially independent of decreased BMD measured by DXA: the OFELY study. J Bone Miner Res. 2007; 22(3):425–33. [PubMed: 17181395]
14. Vilayphiou N, Boutroy S, Szulc P, van Rietbergen B, Munoz F, Delmas PD, Chapurlat R. Finite element analysis performed on radius and tibia HR-pQCT images and fragility fractures at all sites in men. J Bone Miner Res. 2011; 26(5):965–73. [PubMed: 21541999]
15. Johansson L, Sundh D, Zoulakis M, Rudang R, Darelid A, Brisby H, Nilsson AG, Mellstrom D, Lorentzon M. The Prevalence of Vertebral Fractures Is Associated With Reduced Hip Bone Density and Inferior Peripheral Appendicular Volumetric Bone Density and Structure in Older Women. J Bone Miner Res. 2017
16. Rudang R, Darelid A, Nilsson M, Mellstrom D, Ohlsson C, Lorentzon M. X-ray-verified fractures are associated with finite element analysis-derived bone strength and trabecular microstructure in young adult men. J Bone Miner Res. 2013; 28(11):2305–16. [PubMed: 23658040]
17. Szulc P, Boutroy S, Vilayphiou N, Chaitou A, Delmas PD, Chapurlat R. Cross-sectional analysis of the association between fragility fractures and bone microarchitecture in older men: the STRAMBO study. J Bone Miner Res. 2011; 26(6):1358–67. [PubMed: 21611974]
18. Blank JB, Cawthon PM, Carrion-Petersen ML, Harper L, Johnson JP, Mitson E, Delay RR. Overview of recruitment for the osteoporotic fractures in men study (MrOS). Contemp Clin Trials. 2005; 26(5):557–568. [PubMed: 16085466]
19. Orwoll E, Blank JB, Barrett-Connor E, Cauley J, Cummings S, Ensrud K, Lewis C, Cawthon PM, Marcus R, Marshall LM, McGowan J, Phipps K, Sherman S, Stefanick ML, Stone K. Design and baseline characteristics of the osteoporotic fractures in men (MrOS) study--a large observational study of the determinants of fracture in older men. Contemp Clin Trials. 2005; 26(5):569–585. [PubMed: 16084776]
20. Manske SL, Zhu Y, Sandino C, Boyd SK. Human trabecular bone microarchitecture can be assessed independently of density with second generation HR-pQCT. Bone. 2015; 79:213–21. [PubMed: 26079995]
21. Bonaretti S, Vilayphiou N, Chan CM, Yu A, Nishiyama K, Liu D, Boutroy S, Ghasem-Zadeh A, Boyd SK, Chapurlat R, McKay H, Shane E, Bouxsein ML, Black DM, Majumdar S, Orwoll ES, Lang TF, Khosla S, Burghardt AJ. Operator variability in scan positioning is a major component of HR-pQCT precision error and is reduced by standardized training. Osteoporos Int. 2017; 28(1): 245–257. [PubMed: 27475931]
22. Pialat JB, Burghardt AJ, Sode M, Link TM, Majumdar S. Visual grading of motion induced image degradation in high resolution peripheral computed tomography: impact of image quality on measures of bone density and micro-architecture. Bone. 2012; 50(1):111–8. [PubMed: 22019605]

23. Burghardt AJ, Pialat JB, Kazakia GJ, Boutroy S, Engelke K, Patsch JM, Valentinitsch A, Liu D, Szabo E, Bogado CE, Zanchetta MB, McKay HA, Shane E, Boyd SK, Bouxsein ML, Chapurlat R, Khosla S, Majumdar S. Multicenter precision of cortical and trabecular bone quality measures assessed by high-resolution peripheral quantitative computed tomography. J Bone Miner Res. 2013; 28(3):524–36. [PubMed: 23074145]

24. Van Rietbergen B, Odgaard A, Kabel J, Huiskes R. Direct mechanics assessment of elastic symmetries and properties of trabecular bone architecture. J Biomech. 1996; 29(12):1653–7. [PubMed: 8945668]

25. Mueller TL, Christen D, Sandercott S, Boyd SK, van Rietbergen B, Eckstein F, Lochmuller EM, Muller R, van Lenthe GH. Computational finite element bone mechanics accurately predicts mechanical competence in the human radius of an elderly population. Bone. 2011; 48(6):1232–8. [PubMed: 21376150]

26. Genant HK, Wu CY, van Kuijk C, Nevitt MC. Vertebral fracture assessment using a semiquantitative technique. J Bone Miner Res. 1993; 8(9):1137–1148. [PubMed: 8237484]

27. Washburn RA, Smith KW, Jette AM, Janney CA. The Physical Activity Scale for the Elderly (PASE): development and evaluation. J Clin Epidemiol. 1993; 46(2):153–162. [PubMed: 8437031]

28. Ohlsson C, Sundh D, Wallerek A, Nilsson M, Karlsson M, Johansson H, Mellstrom D, Lorentzon M. Cortical Bone Area Predicts Incident Fractures Independently of Areal Bone Mineral Density in Older Men. J Clin Endocrinol Metab. 2017; 102(2):516–524. [PubMed: 27875059]

29. Biver E, Durosier-Izart C, Chevalley T, van Rietbergen B, Rizzoli R, Ferrari S. Evaluation of Radius Microstructure and Areal Bone Mineral Density Improves Fracture Prediction in Postmenopausal Women. J Bone Miner Res. 2017

30. Sornay-Rendu E, Boutroy S, Duboeuf F, Chapurlat RD. Bone Microarchitecture Assessed by HR-pQCT as Predictor of Fracture Risk in Postmenopausal Women: The OFELY Study. J Bone Miner Res. 2017; 32(6):1243–1251. [PubMed: 28276092]

31. Langsetmo L, Peters KW, Burghardt AJ, Ensrud KE, Fink HA, Cawthon PM, Cauley JA, Schousboe JT, Barrett-Connor E, Orwoll ES, Osteoporotic G. Fractures in Men Study Research. Volumetric Bone Mineral Density and Failure Load of Distal Limbs Predict Incident Clinical Fracture Independent of FRAX and Clinical Risk Factors Among Older Men. J Bone Miner Res. 2018

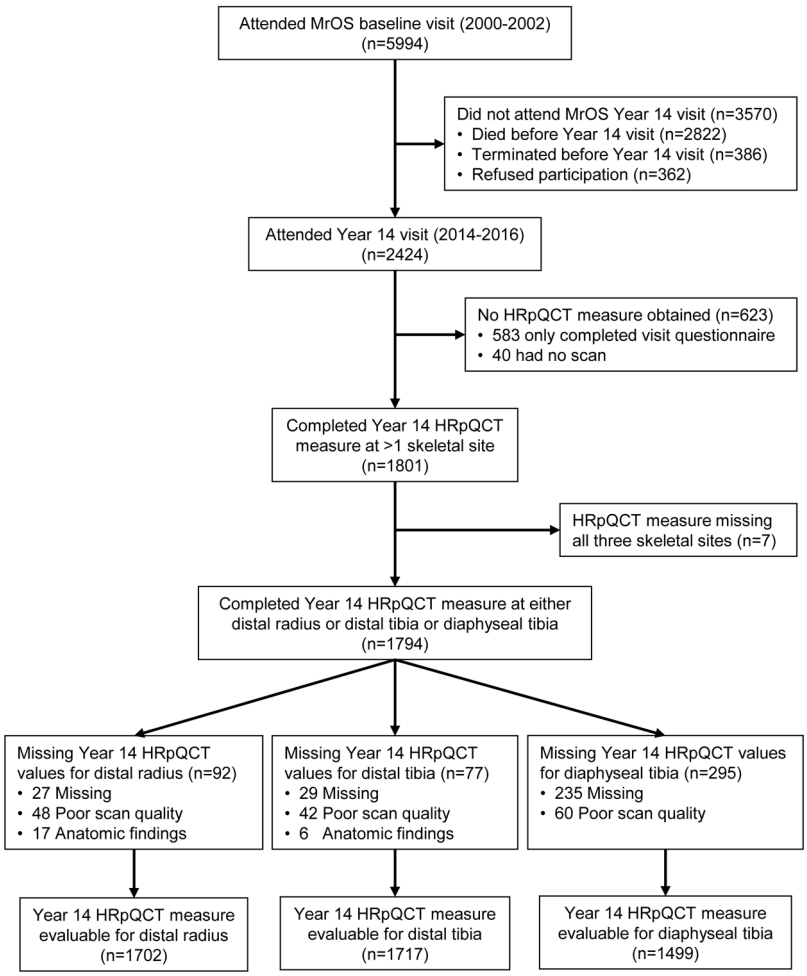

Figure 1.
Analysis Cohort

Table 1

Comparison of Year 14 study visit characteristics between men in HR-pQCT analysis cohort with and without confirmed clinical fracture between MrOS baseline and Year 14 visit

Characteristic	No confirmed clinical fracture between baseline and Y14 visit N=1450	Confirmed clinical fracture between baseline and Y14 visit N=344	P-value*
Age (years), mean (SD)	84.3 (4.2)	85.0 (4.2)	<0.01
Race (white), n (%)	1301 (89.7)	320 (93.0)	0.06
Height (cm), mean (SD)	172.2 (6.8)	172.4 (7.0)	0.56
Weight (kg), mean (SD)	79.9 (12.6)	79.4 (12.4)	0.51
Physical activity (PASE score), mean (SD)	116.1 (65.3)	105.1 (68.4)	<0.01
Smoking status, n (%)			0.02
Never	642 (44.3)	129 (37.5)	
Past/Current	807 (55.7)	215 (62.5)	
Current alcohol consumption, n (%)			0.67
None to <1 drink/week	735 (51.1)	166 (48.4)	
1–13 drinks/week	638 (44.3)	161 (46.9)	
≥14 drinks/week	66 (4.6)	16 (4.7)	
Any fall in past year, n (%)	515 (35.6)	175 (50.9)	<0.01
Total hip aBMD, mean (SD)	0.944 (0.151)	0.880 (0.138)	<0.01
Self-reported fracture between age 50 and baseline, n (%)	254 (17.6)	106 (30.8)	<0.01
Radius length (mm), mean (SD)	286.0 (14.7)	287.8 (14.9)	0.06
Tibia length (mm), mean (SD)	403.5 (24.4)	407.7 (26.7)	<0.01

Y14 = MrOS Year 14 study visit; HR-pQCT = high-resolution peripheral computed tomography; SD = standard deviation; PASE = Physical Activity Scale for the Elderly; aBMD = areal bone mineral density

*t-test for continuous variables and chi-square test for categorical variables

Table 2

Association of Year 14 HR-pQCT microarchitectural parameters with history of prior clinical fracture between MrOS baseline and Year 14 study visits, Odds Ratio (95% CI)

	Per 1 unit SD decrement	Model 1	Model 2	Model 3
Distal Radius		n-used=1702 *n-event=318*	n-used=1657 *n-event=300*	n-used=1639 *n-event=298*
FEA estimated failure load, N	1338.1 N	1.62 (1.41, 1.86)	1.36 (1.15, 1.62)	1.35 (1.14, 1.60)
Total vBMD, mg/cm^3	61.2 mg/cm^3	1.52 (1.32, 1.74)	1.24 (1.06, 1.46)	1.22 (1.03, 1.44)
Total bone area, mm^2	66.3 mm^2	0.98 (0.85, 1.12)	1.00 (0.86, 1.15)	1.02 (0.88, 1.18)
Trabecular vBMD, mg/cm^3	39.4 mg/cm^3	1.46 (1.28, 1.66)	1.19 (1.02, 1.39)	1.17 (1.00, 1.38)
Trabecular number, mm^{-1}	0.21 mm^{-1}	1.40 (1.24, 1.59)	1.17 (1.00, 1.36)	1.16 (1.00, 1.35)
Trabecular thickness, mm	0.018 mm	1.19 (1.05, 1.35)	1.04 (0.91, 1.19)	1.03 (0.90, 1.19)
Trabecular bone area, mm^2	68.3 mm^2	0.90 (0.78, 1.02)	0.95 (0.83, 1.09)	0.97 (0.83, 1.12)
Cortical vBMD, mg/cm^3	69.2 mg/cm^3	1.34 (1.18, 1.52)	1.21 (1.06, 1.39)	1.18 (1.03, 1.36)
Cortical porosity, %	0.81%	1.13 (0.99, 1.28)	1.05 (0.92, 1.19)	1.06 (0.93, 1.22)
Cortical thickness, mm	0.230 mm	1.45 (1.27, 1.66)	1.25 (1.07, 1.45)	1.23 (1.06, 1.44)
Cortical bone area, mm^2	14.3 mm^2	1.50 (1.31, 1.73)	1.30 (1.11, 1.52)	1.30 (1.11, 1.53)
Distal Tibia		n-used=1717 *n-event=326*	n-used=1678 *n-event=311*	n-used=1660 *n-event=309*
FEA estimated failure load, N	2934.3 N	1.61 (1.40, 1.84)	1.32 (1.10, 1.57)	1.26 (1.05, 1.51)
Total vBMD, mg/cm^3	55.2 mg/cm^3	1.53 (1.34, 1.76)	1.24 (1.04, 1.47)	1.20 (1.01, 1.43)
Total bone area, mm^2	136.9 mm^2	0.94 (0.81, 1.08)	0.93 (0.80, 1.08)	0.92 (0.78, 1.08)
Trabecular vBMD, mg/cm^3	38.1 mg/cm^3	1.29 (1.14, 1.47)	1.02 (0.88, 1.19)	1.00 (0.86, 1.17)
Trabecular number, mm^{-1}	0.213 mm^{-1}	1.19 (1.05, 1.34)	0.97 (0.84, 1.12)	0.97 (0.84, 1.12)
Trabecular thickness, mm	0.023 mm	1.09 (0.96, 1.24)	1.00 (0.87, 1.14)	0.99 (0.86, 1.14)
Trabecular bone area, mm^2	145.7 mm^2	0.84 (0.73, 0.97)	0.89 (0.77, 1.03)	0.88 (0.75, 1.03)
Cortical vBMD, mg/cm^3	80.8 mg/cm^3	1.48 (1.30, 1.67)	1.30 (1.12, 1.50)	1.26 (1.09, 1.46)
Cortical porosity, %	1.65%	0.95 (0.84, 1.07)	0.94 (0.83, 1.07)	0.96 (0.84, 1.09)
Cortical thickness, mm	0.335 mm	1.48 (1.29, 1.70)	1.24 (1.07, 1.45)	1.23 (1.05, 1.44)

	Per 1 unit SD decrement	Model 1	Model 2	Model 3
Cortical bone area, mm^2	31.1 mm^2	1.50 (1.32, 1.71)	1.28 (1.09, 1.49)	1.26 (1.08, 1.47)
Diaphyseal Tibia		n-used=1499 *n-event=268*	n-used=1465 *n-event=253*	n-used=1449 *n-event=252*
FEA estimated failure load, N	2703.3 N	1.61 (1.38, 1.87)	1.39 (1.17, 1.65)	1.35 (1.12, 1.62)
Total vBMD, mg/cm^3	78.6 mg/cm^3	1.30 (1.14, 1.49)	1.06 (0.90, 1.24)	1.03 (0.88, 1.22)
Total bone area, mm^2	51.7 mm^2	1.20 (1.03, 1.39)	1.17 (1.00, 1.37)	1.18 (1.00, 1.40)
Cortical vBMD, mg/cm^3	35.0 mg/cm^3	1.10 (0.96, 1.26)	0.99 (0.86, 1.14)	0.96 (0.82, 1.12)
Cortical bone area, mm^2	40.3 mm^2	1.58 (1.36, 1.84)	1.38 (1.15, 1.64)	1.35 (1.12, 1.62)
Cortical porosity, %	1.18%	0.85 (0.75, 0.96)	0.93 (0.81, 1.06)	0.95 (0.83, 1.09)
Cortical thickness, mm	0.881 mm	1.43 (1.24, 1.65)	1.21 (1.02, 1.43)	1.17 (0.99, 1.39)

Y14 = MrOS Year 14 study visit; HR-pQCT = high resolution peripheral quantitative computed tomography; OR = odds ratio; CI = confidence intervals, SD = standard deviation; FEA = finite element analysis; aBMD = areal bone mineral density; vBMD = volumetric bone mineral density; n-used = number of men

Model 1 adjusted for Y14 age, race, limb length and clinic site

Model 2 adjusted for Y14 age, race, limb length, clinic site and DXA total hip aBMD

Model 3 adjusted for Y14 age, race, clinic site, limb length, weight, physical activity, baseline smoking status, alcohol consumption, past falls, self-reported history of fracture between age 50 and MrOS baseline, and DXA total hip aBMD

Table 3

Association of Year 14 HR-pQCT microarchitectural parameters with history of prior major osteoporotic fracture between MrOS baseline and Year 14 study visits, Odds Ratio (95% CI)

	Per 1 SD decrease unit	Model 1	Model 2	Model 3
Distal Radius		n-used=1702 *n-event=104*	n-used=1657 *n-event=98*	n-used=1639 *n-event=98*
FEA estimated failure load, N	1338.1 N	1.74 (1.38, 2.20)	1.44 (1.09, 1.90)	1.43 (1.08, 1.90)
Total vBMD, mg/cm^3	61.2 mg/cm^3	1.82 (1.45, 2.30)	1.54 (1.17, 2.02)	1.49 (1.12, 1.96)
Total bone area, mm^2	66.3 mm^2	0.76 (0.61, 0.94)	0.75 (0.60, 0.93)	0.78 (0.62, 0.99)
Trabecular vBMD, mg/cm^3	39.4 mg/cm^3	1.88 (1.50, 2.35)	1.65 (1.26, 2.14)	1.61 (1.23, 2.11)
Trabecular number, mm^{-1}	0.21 mm^{-1}	1.75 (1.44, 2.13)	1.53 (1.21, 1.93)	1.52 (1.20, 1.92)
Trabecular thickness, mm	0.018 mm	1.20 (0.97, 1.48)	1.09 (0.87, 1.36)	1.06 (0.84, 1.34)
Trabecular bone area, mm^2	68.3 mm^2	0.71 (0.58, 0.88)	0.74 (0.59, 0.92)	0.77 (0.61, 0.98)
Cortical vBMD, mg/cm^3	69.2 mg/cm^3	1.34 (1.10, 1.63)	1.16 (0.94, 1.44)	1.13 (0.91, 1.41)
Cortical porosity, %	0.81%	1.46 (1.16, 1.85)	1.37 (1.08, 1.75)	1.38 (1.08, 1.76)
Cortical thickness, mm	0.230 mm	1.56 (1.24, 1.95)	1.32 (1.03, 1.70)	1.28 (0.99, 1.66)
Cortical bone area, mm^2	14.3 mm^2	1.40 (1.12, 1.76)	1.13 (0.88, 1.46)	1.13 (0.87, 1.47)
Distal Tibia		n-used=1717 *n-event=115*	n-used=1678 *n-event=109*	n-used=1660 *n-event=109*
FEA estimated failure load, N	2934.3 N	1.94 (1.55, 2.42)	1.51 (1.13, 2.02)	1.50 (1.11, 2.01)
Total vBMD, mg/cm^3	55.2 mg/cm^3	1.89 (1.52, 2.36)	1.47 (1.11, 1.94)	1.38 (1.04, 1.82)
Total bone area, mm^2	136.9 mm^2	0.78 (0.63, 0.98)	0.77 (0.61, 0.98)	0.80 (0.63, 1.03)
Trabecular vBMD, mg/cm^3	38.1 mg/cm^3	1.53 (1.25, 1.88)	1.16 (0.91, 1.48)	1.10 (0.86, 1.41)
Trabecular number, mm^{-1}	0.213 mm^{-1}	1.19 (0.98, 1.44)	0.89 (0.71, 1.11)	0.86 (0.69, 1.08)
Trabecular thickness, mm	0.023 mm	1.20 (0.98, 1.47)	1.07 (0.86, 1.32)	1.03 (0.83, 1.29)
Trabecular bone area, mm^2	145.7 mm^2	0.69 (0.55, 0.87)	0.74 (0.59, 0.94)	0.77 (0.60, 0.98)
Cortical vBMD, mg/cm^3	80.8 mg/cm^3	1.49 (1.23, 1.81)	1.23 (0.99, 1.53)	1.21 (0.96, 1.51)
Cortical porosity, %	1.65%	1.14 (0.93, 1.39)	1.12 (0.92, 1.37)	1.15 (0.93, 1.41)
Cortical thickness, mm	0.335 mm	1.74 (1.40, 2.15)	1.40 (1.09, 1.78)	1.38 (1.08, 1.77)

	Per 1 SD decrease unit	Model 1	Model 2	Model 3
Cortical bone area, mm^2	31.1 mm^2	1.63 (1.34, 2.01)	1.30 (1.03, 1.65)	1.31 (1.03, 1.68)
Diaphyseal Tibia		n-used=1499 *n-event=98*	n-used=1465 *n-event=92*	n-used=1449 *n-event=92*
FEA estimated failure load, N	2703.3 N	1.60 (1.27, 2.00)	1.23 (0.94, 1.62)	1.25 (0.94, 1.65)
Total vBMD, mg/cm^3	78.6 mg/cm^3	1.19 (0.97, 1.46)	0.88 (0.69, 1.12)	0.83 (0.64, 1.06)
Total bone area, mm^2	51.7 mm^2	1.35 (1.07, 1.71)	1.28 (1.00, 1.64)	1.42 (1.09, 1.86)
Cortical vBMD, mg/cm^3	35.0 mg/cm^3	1.12 (0.91, 1.37)	0.95 (0.77, 1.19)	0.88 (0.70, 1.12)
Cortical porosity, %	1.18%	0.87 (0.72, 1.04)	0.98 (0.80, 1.19)	1.02 (0.84, 1.26)
Cortical thickness, mm	0.881 mm	1.27 (1.03, 1.57)	0.93 (0.72, 1.21)	0.92 (0.71, 1.19)
Cortical bone area, mm^2	40.3 mm^2	1.54 (1.22, 1.93)	1.20 (0.91, 1.57)	1.23 (0.93, 1.63)

Model 1 adjusted for V4 age, race, limb length and clinic site

Model 2 adjusted for V4 age, race, limb length, clinic site and V4 total hip BMD

Model 3 adjusted for V4 age, race, clinic site, limb length, weight, physical activity, baseline smoking status, alcohol consumption, past falls, self-reported history of fracture between age 50 and MrOS baseline, and V4 total hip BMD